

Featured Article

Exploiting Chitin as a Source of Biologically Fixed Nitrogen: Formation and Full Characterization of Small Molecule Hetero- and Carbo-Cyclic Pyrolysis Products

Maryam Nikahd, Jiri Mikusek, Li-Juan Yu, Michelle L. Coote,
Martin G Banwell, Chenxi Ma, and Michael G Gardiner

J. Org. Chem., **Just Accepted Manuscript** • DOI: 10.1021/acs.joc.9b03438 • Publication Date (Web): 05 Feb 2020

Downloaded from pubs.acs.org on February 5, 2020

Just Accepted

“Just Accepted” manuscripts have been peer-reviewed and accepted for publication. They are posted online prior to technical editing, formatting for publication and author proofing. The American Chemical Society provides “Just Accepted” as a service to the research community to expedite the dissemination of scientific material as soon as possible after acceptance. “Just Accepted” manuscripts appear in full in PDF format accompanied by an HTML abstract. “Just Accepted” manuscripts have been fully peer reviewed, but should not be considered the official version of record. They are citable by the Digital Object Identifier (DOI®). “Just Accepted” is an optional service offered to authors. Therefore, the “Just Accepted” Web site may not include all articles that will be published in the journal. After a manuscript is technically edited and formatted, it will be removed from the “Just Accepted” Web site and published as an ASAP article. Note that technical editing may introduce minor changes to the manuscript text and/or graphics which could affect content, and all legal disclaimers and ethical guidelines that apply to the journal pertain. ACS cannot be held responsible for errors or consequences arising from the use of information contained in these “Just Accepted” manuscripts.

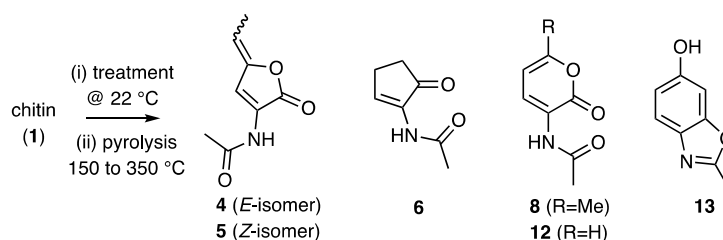
1
2
3 **Exploiting Chitin as a Source of Biologically Fixed Nitrogen:**
4 **Formation and Full Characterization of Small Molecule**
5 **Hetero- and Carbo-Cyclic Pyrolysis Products**
6
7

8 Maryam Nikahd,[†] Jiri Mikusek,[†] Li-Juan Yu,^{†,§} Michelle L. Coote,^{†,§}
9 Martin G. Banwell,^{*,†,‡} Chenxi Ma[†] and Michael G. Gardiner[†]
10
11

12 [†]Research School of Chemistry, Institute of Advanced Studies
13 The Australian National University, Canberra, ACT 2601, Australia
14
15

16 [§] ARC Centre of Excellence for Electromaterials Science, Research School of
17 Chemistry,
18 The Australian National University, Canberra, ACT 2601, Australia
19
20

21 [‡]Institute for Advanced and Applied Chemical Synthesis,
22 Jinan University, Guangzhou 510632, China
23
24
25
26
27



37 **Abstract:** Pyrolysis of variously pre-treated or untreated samples of chitin (**1**) and certain
38 congeners at 150–350 °C afforded a range of platform molecules, as exemplified by
39 compounds **4**, **5**, **6**, **8**, **12** and **13**. All of these products have been fully characterized,
40 including by single-crystal X-ray analysis. Pathways for the formation of them are
41 proposed and theoretical studies of certain aspects of these described.
42
43

44 **INTRODUCTION**

45 Chitin (**1**, Figure 1), which is comprised of linearly-linked repeating units of *N*-
46 acetylglucosamine (NAG, **2**), is an abundant biopolymer that is found in the exoskeleta of
47 crustaceans, the cuticles of insects, plankton and the cell walls of fungi. It has been
48 estimated that such organisms produce ca. 100 billion tons annually.¹ Unlike its even more
49 common counterpart cellulose (**3**), chitin is a source of biologically-fixed nitrogen and
50 has thus attracted interest as a potential precursor, through thermally-promoted
51 depolymerization processes, to small organic molecules that contain this heteroatom.
52 Such compounds, that are otherwise known as biomass-derived platform molecules,²
53 could serve, for example, as sustainably-produced building blocks for chemical synthesis.
54 Such possibilities have attracted some attention, particularly in more recent times, and a
55 range of such depolymerization products has been observed,³ one of which was employed
56 in chemical syntheses.⁴
57
58
59
60

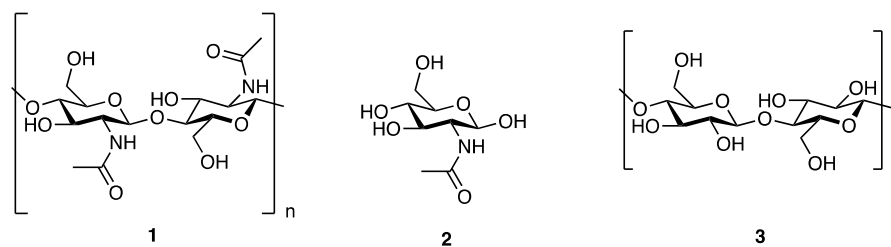


Figure 1: The structures of chitin (1), NAG (2) and cellulose (3)

Our ongoing interest⁵ in exploiting the small molecule products arising from the pyrolytic depolymerization of acid-treated cellulose,⁶ most particularly levoglucosenone and its hydrogenation product CyreneTM (now marketed as a replacement for the industrial solvent NMP),⁷ have prompted us to examine the outcomes of applying similar conditions to chitin. The results of such studies are reported here and reveal that a plethora of small molecule, nitrogen-containing reaction products (Figure 2), including previously unreported ones, can be obtained by pyrolysis. The distribution of such products appears to be influenced significantly by the way in which chitin is treated prior to pyrolysis. Reaction pathways for the formation of these products are advanced and theoretical support for some of these are also presented.

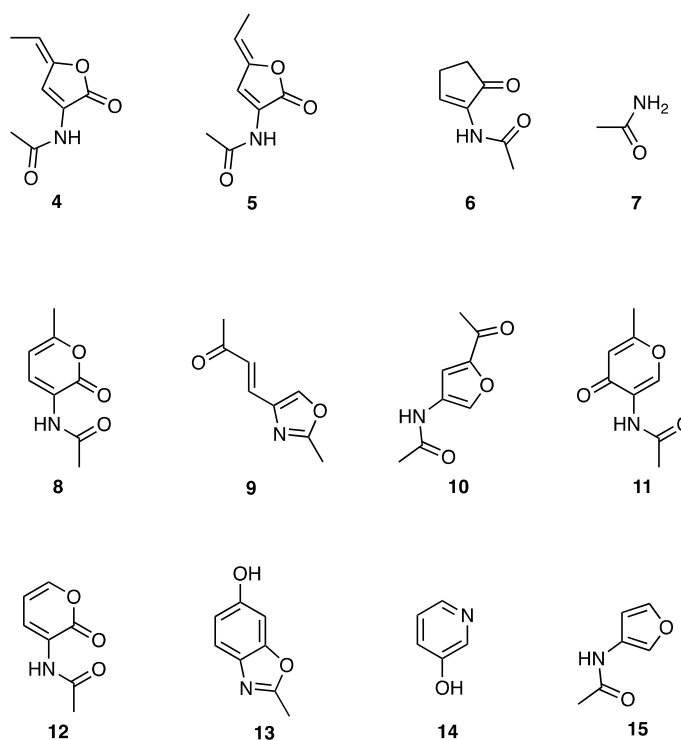


Figure 2: Structures of the products, 4-15, arising from pyrolysis of pre-treated and untreated chitin (1), chitosan and/or NAG (2).

RESULTS AND DISCUSSION

Initial chitin pyrolysis experiments (Entry 1, Table 1) were conducted by external heating of untreated and commercially supplied chitin placed in a glass vessel under reduced pressure (5 mbar) at 300-350 °C for 1.0 h (see Experimental Section and Supporting Information – SI – for full details).⁸ The condensate collected at liquid nitrogen

temperatures was combined with the methanolic washings of the residue remaining in the pyrolysis zone and this mixture then subjected to chromatographic fractionation. By such means small amounts of compounds **4**, **5** and **6** were obtained with each being fully characterized by spectroscopic methods including, in the case of the first and third of these, single-crystal X-ray analysis (see SI for details). Under such conditions, and in every other instance as well, significant quantities (normally > 50%) of acetamide (**7**) were also observed and the structure of this confirmed by both single-crystal X-ray analysis and spectroscopic comparisons with an authentic sample. Conventional spectroscopic analysis of the methanol-washed and dried residue (comprising up to 50% of the original mass of chitin) suggested it was a complex mixture of oligomeric materials that we have not investigated further at this stage.

Table 1: Products observed from pyrolysis of pre-treated and untreated chitin (**1**), chitosan (*N*-deacyl-**2**) and NAG (**2**).

Entry	Substrate	Pre-treatment	Pyrolysis conditions	Products ^a
1	chitin	none	300-350 °C/1.0 h	4, 5, 6, 7
2	chitin	3% aq. H ₃ PO ₄	200-350 °C/1.5 to 6 h	4, 5, 6, 7, 8, 9
3	chitin	glacial AcOH	350 °C/1.5 to 2 h	6, 7, 8, 9, 12, 13
4	chitin	40% aq. glyoxal	250 °C/2 h	levoglucosenone, 7
5	chitosan	none	350 °C/1.5 h	6, 7, 10, 11, 14
6	NAG	none	350 °C/1.5 h	7, 10
7	NAG	Na ₂ HPO ₄	150-300 °C/1.5 h	7, 10, 15

^a The quantities of the products obtained from the various pyrolysis experiments involved are given in the Experimental Section. Acetamide (**7**) was always the dominant product and could be obtained in up to 90% yield.

Pyrolysis of chitin under the same conditions as detailed above but that had now been pre-treated with 3% aqueous phosphoric acid at ambient temperatures for various periods of time (5 min to 72 h) before being dried (to a free flowing powder) provided (Entry 2, Table 1) not only the previously observed products (viz. **4-7**) in similar yields but, in addition, the *2H*-pyran-2-one **8** and oxazole **9**. The structures of these last two compounds were also confirmed by single-crystal X-ray analysis. Interestingly, when chitin was pre-treated with glacial acetic acid rather than phosphoric acid (and the ensuing mixture then dried prior to pyrolysis), new, small-molecule breakdown products were observed (Entry 3, Table 1). In particular, *2H*-pyran-2-one **12** and benzo[*d*]oxazole **13** were now obtained (and the structures of these also confirmed by single-crystal X-ray analysis) along with the previously observed products **6-9**. Chitin was also treated with 40% aqueous glyoxal solution and the resulting mixture then dried prior to pyrolysis. Under the usual pyrolytic conditions (Entry 4, Table 1) such pre-treated material once again afforded acetamide (**7**) as the major product with the only other isolable and fully characterizable small-molecule product now being levoglucosenone.

The polymer chitosan (*N*-deacetylchitin) is derived from chitin through treatment with alkali, a process purported to remove the associated acetyl groups and so producing a linear polymer of glucosamine. However, subjecting commercially acquired chitosan to essentially the same pyrolytic conditions (Entry 5, Table 1) as employed before gave small amounts of the previously observed *N*-acetyl-containing compounds **6** and **7** as well as furan **10** and *4H*-pyran-4-one **11**. Once again, the structures of these last two

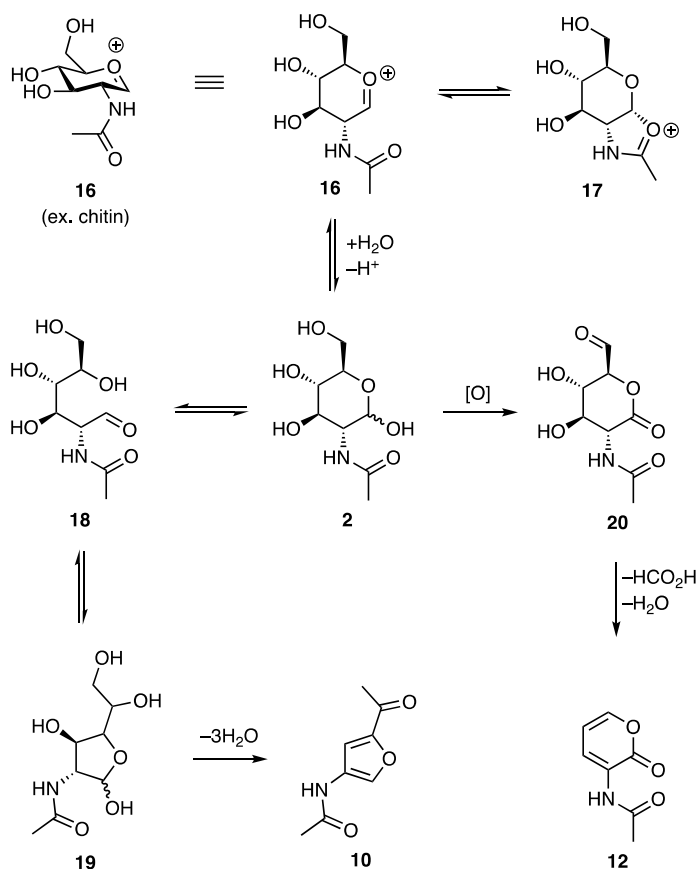
1
2
3 compounds were confirmed by single-crystal X-ray analysis. Another product of this
4 process was 3-hydroxypyridine (**14**) that could only be characterized by single-crystal X-
5 ray analysis of its trifluoroacetate salt (formed as a result of using trifluoroacetic acid as a
6 solvent in part of an HPLC purification process). Presumably the *N*-acylated products
7 arise through pyrolysis of the residual chitin contained within the sample of chitosan
8 employed.
9

10
11 Pyrolysis of untreated NAG (Entry 6, Table 1) gave just two isolable products, namely
12 acetamide (**7**) and the previously observed furan **10**. Pre-treatment of NAG with
13 Na₂HPO₄ prior to its pyrolysis also gave compounds **7** and **10** but these were now
14 accompanied by the deacylated counterpart of the latter, namely compound **15** and the
15 structure of which was also established by single-crystal X-ray analysis.
16
17

18 Only one member of the suite of cyclic products obtained from the above-mentioned
19 pyrolyses has been isolated and fully characterized previously. Thus, the disubstituted
20 furan **10** has been reported^{3a-c} as a major pyrolysis product and exploited as a starting
21 material in chemical syntheses.⁴ Intriguingly, compound **10** has also been isolated from
22 the whole bodies of *Polyphaga plancyi* Bolivar,⁹ an insect widely distributed in China. In
23 1984 Franich and co-workers suggested,¹⁰ based on mass spectrometric analyses, that
24 compounds **8** and **11** are formed by pyrolysis of NAG. More recently, Wu's group has
25 suggested^{3e} that furan **15** is obtained from the "fast" pyrolysis of chitin but only appear to
26 base this claim on GC/MS data. Interestingly, using the same analytical technique,
27 Stankiewicz et al have suggested¹¹ that compounds **8**, **11** and **15** are formed through the
28 biodegradation of the chitin-protein complex contained within in crustacean cuticle.
29 Certain of the other cyclic products obtained here, namely **6**,¹² **12**,¹³ **13**¹⁴ and **14**,¹⁵ have
30 also been obtained by chemical synthesis but the remaining ones, viz. **4**, **5** and **9**, have not
31 been described in the literature. Further, while pyrazines have been reported^{3e} as
32 significant products from the high temperature (600 °C) pyrolysis of chitin no obvious
33 formation of such compounds was observed in the present study, an outcome we attribute
34 to the milder conditions involved.
35
36
37
38

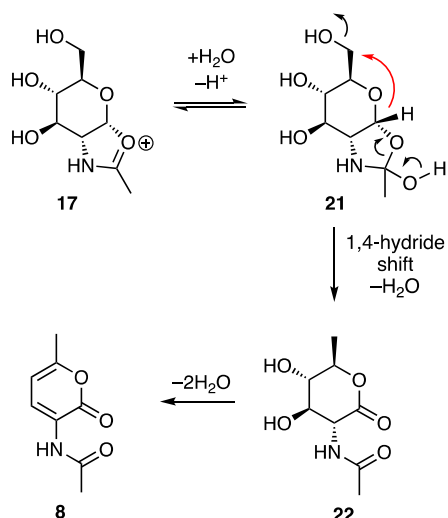
39 From a mechanistic point-of-view, the formation of platform molecules **4-6** and **8-15**
40 from chitin (**1**) almost certainly commences with cleavage of the associated glycosidic
41 bond so as to form the oxonium ion **16** (Scheme 1), a species also likely to be obtained
42 from NAG (**3**) and stabilized through participation of the adjacent (neighboring)
43 acetamido group via formation of isomer **17**.
44
45
46
47
48
49
50
51
52
53
54
55
56
57
58
59
60

Scheme 1: Possible intermediates arising from the pyrolysis of chitin (**1**) or NAG (**2**) and their conversion into products **10** and **12**.

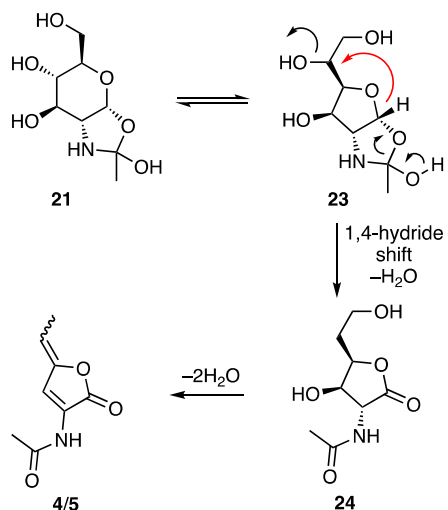


In keeping with earlier proposals,^{3b} we suggest cation **16** would be readily converted into NAG (**2**) and that the open-chain form of this (**18**) cyclizes to give the corresponding furanose **19**, three-fold dehydration of which would afford the observed and disubstituted furan **10**. Given the structural relationship between this product and its mono-substituted and co-produced counterpart **15**, we believe this is formed by C2-deacylation rather than through a retro-Diels-Alder reaction as proposed by Wu.^{3e} In an alternative reaction pathway, selective oxidation of NAG could give the lactone-aldehyde **20** that might be expected to lose the elements formic acid and water (no order implied) and thereby forming the observed 2*H*-pyran-2-one **12**.

A possible but distinct pathway for the formation of the related 2*H*-pyran-2-one **8** is shown in Scheme 2 and would involve the conversion of cation **17** into the oxazolidin-2-ol **21** that itself fragments with an accompanying 1,4-hydride shift¹⁶ (see red arrow) across the β -face of the pyranose framework and loss of water to afford the C6-deoxygenated lactone **22** that itself undergoes two-fold dehydration to give the observed product **8**.

Scheme 2: A possible pathway from cation **17** to pyrolysis product **8**.

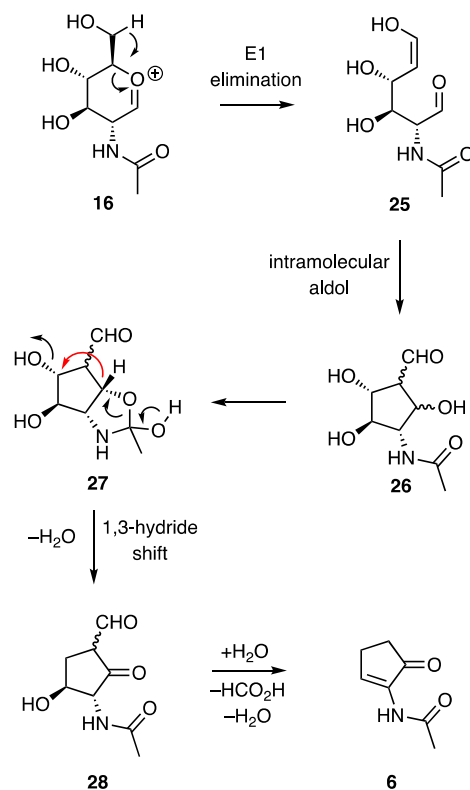
A related pathway for the formation of the isomeric furanolactones **4** and **5** is shown in Scheme 3. Specifically, conversion of compound **21** into isomer **23** followed by a 1,4-hydride shift (see red arrow) within the latter species (cf **21** \rightarrow **22** in Scheme 2) could deliver the dihydroxylated furanone **24** that upon two-fold dehydration would afford compounds **4** and **5**. A high-level ab initio molecular orbital theory study of the 1,4-hydride shifts proposed in the Schemes 2 and 3 revealed the energetically feasible nature of these processes and suggests each proceeds in a stepwise manner and involves the intermediacy of a bridging water molecule (see the SI for details).

Scheme 3: A possible pathway from compound **21** to pyrolysis products **4** and **5**.

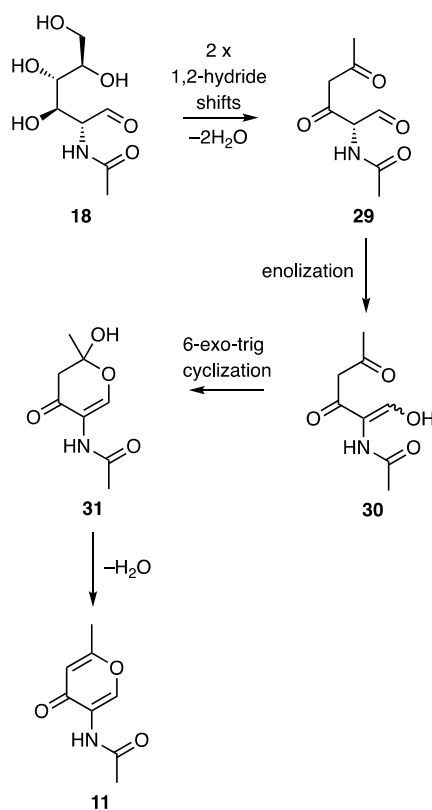
The elimination/intramolecular aldol/1,3-hydride shift sequence shown in Scheme 4 could account for the formation of cyclopentenone **6** from the cation **16**. Thus, an E1 elimination process within the latter species would deliver a product, **25**, primed for an intramolecular aldol reaction and so affording cyclopentane **26** that could isomerize to the oxazolidin-2-ol **27**. A 1,3-hydride shift¹⁷ (see red arrow) and accompanying loss of the elements of water within this last compound would deliver the keto-aldehyde **28** and

subsequent hydration, retro-aldol and dehydration processes could then provide compound **6**.

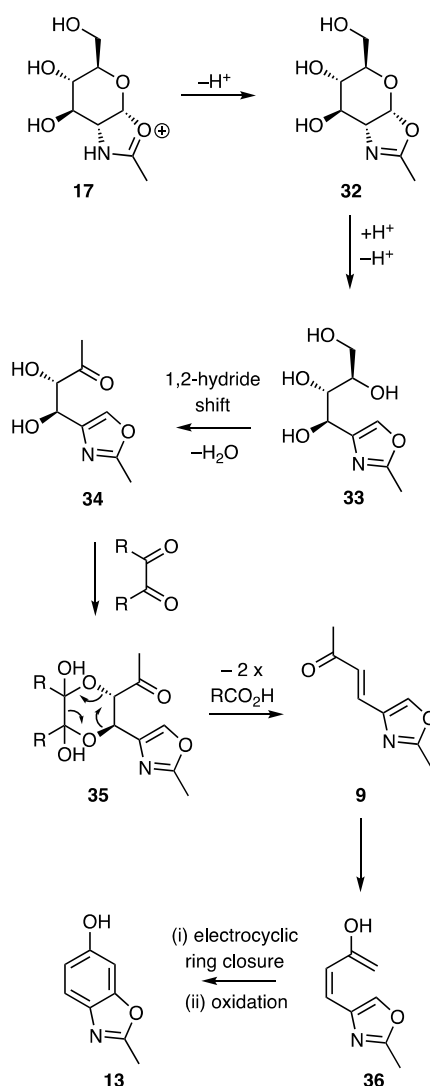
Scheme 4: A possible pathway from cation **16** to cyclopentenone **6**.



The formation of the 4*H*-pyran-4-one **11** could arise, as shown in Scheme 5, through a two-fold 1,2-hydride shift sequence and accompanying dehydration¹⁸ that would deliver compound **29**. Tautomerization of this last species would generate the enol **30**, the *E*-form of which could cyclize in a 6-*exo*-*trig* process to lactol **31** that upon the loss of the elements of water could provide the observed product **11**.

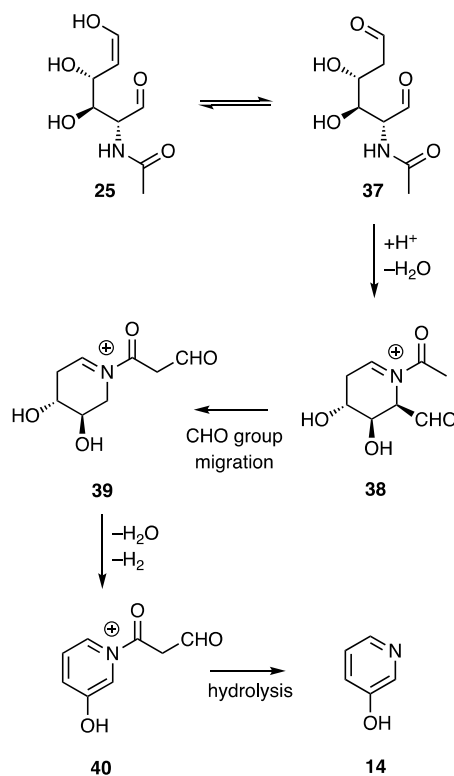
Scheme 5: A pathway from compound **18** to 4*H*-pyran-4-one **11**

Given that each embodies an oxazole ring, the pathways leading to the formation of compounds **9** and **13** are likely to be related (connected) and one such possibility is shown in Scheme 6. Thus, deprotonation of cation **17** followed by acid-catalyzed isomerization of the resulting dihydro-oxazole **32** would afford compound **33** that could undergo a 1,2-hydride shift with accompanying dehydration and so affording the methyl ketone **34**. The necessary loss of the two remaining hydroxyl groups within this last compound presents an interesting conundrum and we speculate that one of various possible α -dicarbonyl compounds that are often observed during the decomposition of monosaccharides (and represented in the general form RCOCOR)¹⁹ could react with the diol residue associated with compound **34** so as to form the bis-lactol **35** that could itself undergo the illustrated fragmentation reaction (with accompanying loss of two molecules of RCO_2H)^{20,21} and thereby producing the observed β -arylated α,β -unsaturated ketone **9**. This product could then rearrange to isomer **36**, a system presumed to be capable of engaging in a thermally-induced 6π -electrocyclic ring closure, the product of which could be expected to oxidize and so form the benzannulated oxazole **13**.

Scheme 6: A possible pathway for the formation of oxazoles **9** and **13** from cation **17**

Scheme 7 depicts a possible pathway for the formation of the final heterocyclic pyrolysis product, namely 3-hydroxypyridine (**14**). Specifically, tautomerisation of the E1 product **25** to the corresponding aldehyde followed by an intramolecular Schiff base condensation reaction might be expected to provide the *N*-acylimminium ion **38**, a species capable of engaging in a formyl group migration reaction that leads to isomer **39** (this conversion may proceed via the corresponding azomethine ylides). Dehydration of diol **39** and accompanying aromatization would then provide the pyridium ion **40** that upon hydrolysis would afford 3-hydroxypyridine (**14**) and malonic semialdehyde (3-oxopropanoic acid – not detected). The HPLC purification process (involving trifluoroacetic acid as a component of the mobile phase) used to isolate product **14** resulted in the formation of its trifluoroacetate salt that proved amenable to single-crystal X-ray analysis (see the SI for details).

Scheme 7: Possible pathway for the conversion of the E1 product **25** into 3-hydroxypyridine (**14**).



The foregoing mechanistic proposals clearly suggest that in almost every instance the acetamido group of chitin and NAG is intimately involved in some way in the formation of the observed pyrolysis products.

CONCLUSION

The present work highlights the diversity of reaction pathways available in the pyrolysis of chitin and the corresponding monomer NAG. Some control over these can be achieved by the manner in which these substrates are treated prior to pyrolysis and the temperatures at which the depolymerization process is conducted. The mechanistic proposals advanced here, and that will be the subject of a range of experiments to be carried out in our laboratories, should help inform how further control can be exerted and so that higher yields of products **4-6** and **8-15** might be realized. As such these biomass-derived platform molecules could assume considerable significance. Compounds **4**, **5**, **8**, **11** and **12**, for example, are dehydro- α -amino acid derivatives and could thus serve as potentially abundant precursors to a range of biologically useful materials.²²

EXPERIMENTAL

General Experimental Protocols

Unless otherwise specified, proton (¹H) and proton-decoupled carbon [¹³C{¹H}] NMR spectra were recorded at room temperature in base-filtered CDCl₃ on a Varian spectrometer operating at 400 MHz for proton and 100 MHz for carbon nuclei. For ¹H NMR spectra, signals arising from the residual protio-forms of the solvent were used as the internal standards. ¹H NMR data are recorded as follows: chemical shift (δ) [multiplicity, coupling constant(s) *J* (Hz), relative integral] where multiplicity is defined as: s = singlet; d = doublet; t = triplet; q = quartet; m = multiplet or combinations of the

1
2
3 above. The signal due to residual CHCl_3 appearing at δ_{H} 7.26 and the central resonance of
4 the CDCl_3 “triplet” appearing at δ_{C} 77.16 were used to reference ^1H and $^{13}\text{C}\{^1\text{H}\}$ NMR
5 spectra, respectively. Infrared spectra (ν_{max}) were recorded on a Perkin–Elmer 1800
6 Series FTIR Spectrometer. Samples were analyzed as thin films. Low-resolution ESI
7 mass spectra were recorded on a single quadrupole liquid chromatograph-mass
8 spectrometer, while high-resolution measurements were conducted on a time-of-flight
9 instrument. Low- and high-resolution EI mass spectra were recorded on a magnetic-sector
10 machine. Melting points were measured on a Reichert melting point microscope and are
11 uncorrected. Analytical thin layer chromatography (TLC) was performed on aluminum-
12 backed 0.2 mm thick silica gel 60 F_{254} plates as supplied by Merck. Eluted plates were
13 visualized using a 254 nm UV lamp and/or by treatment with a suitable dip followed by
14 heating. These dips included phosphomolybdic acid : ceric sulfate : sulfuric acid (conc.) :
15 water (37.5 g : 7.5 g : 37.5 g : 720 mL) or potassium permanganate : potassium carbonate
16 : 5% sodium hydroxide aqueous solution : water (3 g : 20 g : 5 mL : 300 mL). Flash
17 chromatographic separations were carried out following protocols defined by Still *et al.*²³
18 with silica gel 60 (40–63 μm) as the stationary phase and using the AR- or HPLC-grade
19 solvents indicated. Reverse-phase HPLC purifications were carried out using an Alltima
20 C18 250 \times 22 mm column using, as the eluting solvent 3:7 v/v water/acetonitrile at a flow
21 rate of 10 ml/min. and ambient temp. Compounds **4** and **5** were purified using YMC-Pack
22 ODS-AQ, 250 \times 20 mm (P/N 81105) column. Starting materials and reagents were
23 generally available from the Sigma–Aldrich, Merck, TCI, Strem or Lancaster Chemical
24 Companies and were used as supplied. Drying agents and other inorganic salts were
25 purchased from the AJAX, BDH or Unilab Chemical Companies. Tetrahydrofuran
26 (THF), methanol and dichloromethane were dried using a Glass Contour solvent
27 purification system that is based upon a technology originally described by Grubbs *et*
28 *al.*²⁴ Petroleum ether refers to the fraction boiling between 40 and 60 $^{\circ}\text{C}$. Where
29 necessary, reactions were performed under a nitrogen atmosphere.

34 Specific Chemical Transformations

35 Treated or untreated chitin (10.0 g, ex. Aldrich Chemical Co.), either on its own or
36 intimately mixed with acid-washed and chromatography-grade sand (20 g), was loaded
37 into the main chamber of the (Type 1) pyrolysis apparatus shown in Figures S1 and S2.
38 Once the traps had been charged with liquid nitrogen, the pressure in the system was
39 reduced to 5 mm Hg using a standard vacuum pump that was connected via a Schlenk
40 line (vacuum/gas manifold). The exterior surface of the main chamber was then wrapped
41 with electrical heating tape and a current applied via a rheostat such that an external
42 temperature of ca. 150–350 $^{\circ}\text{C}$ was obtained (see Figure S3). Heating was continued for
43 the specified period then the power supply disconnected and once the tape was cool to the
44 touch this was removed and the apparatus opened to the atmosphere. The residue in the
45 pyrolysis chamber (see Figure S4) was washed with methanol, as was the sintered glass
46 frit and glass line leading into the round-bottomed flask that had been sitting in the liquid
47 nitrogen or dry ice and acetone trap. These washings were added into the flask and the
48 resulting mixture concentrated under reduced pressure. The brown oil thus obtained was
49 subjected to flash chromatography (silica gel) under the specified conditions and the
50 relevant fractions subjected, as required, to further purification including, in some
51 instances, using reverse-phase HPLC techniques. In every instance a significant
52 proportion (up 90% yield) of the brown oil was comprised of acetamide (**7**) as determined
53 by NMR and IR spectroscopic as well as mass spectrometric analyses and comparisons
54 with an authentic sample.

55 In another mode (Type 2) of pyrolysis (Figure S5), a round-bottomed flask containing
56 chitin (10 g) (Figure S6) was fitted with a short-path distillation tube that was itself
57
58
59
60

connected to a receiver flask sitting in a liquid nitrogen or dry-ice/acetone bath. The receiver flask was, in turn, connected to a liquid nitrogen trap and, through this, to a Schlenk line by which means the whole apparatus could be evacuated using a vacuum pump. Heat was applied to the reaction flask/chamber by means of an aluminum heating block. To facilitate heat transfer to the contents of the reaction flask either metal ball bearings, canola oil or sand could be mixed with the chitin (see Figure S7). The reaction temperature was held at 150-350 °C for the specified time after which heating was stopped then the cooled apparatus disassembled. The residue in the pyrolysis flask (see Figure S8) was washed with methanol as was the distillation tube leading into the receiver flask. These washings were added into the receiver flask and the resulting mixture concentrated under reduced pressure. The brown oil thus obtained was subjected to flash chromatography (silica gel) under the specified conditions and the relevant fractions subjected, as required, to further purification including, in some instances, using reverse-phase HPLC techniques. In every instance a significant proportion (up 90% yield) of the brown oil was comprised of acetamide (**7**) as determined by NMR and IR spectroscopic as well as mass spectrometric analyses and comparisons with an authentic sample.

(a) Pyrolysis of Untreated Chitin.

Chitin (10.0 g) with or without intimately mixed acid-washed and chromatography-grade sand (20 g), was loaded into the pyrolysis apparatus shown in Figure S1 and with the cold traps in place the pressure in the system was reduced to 5 mm Hg and then heating commenced.

Run #1: No sand, 300 °C, 1 h. The weight of the residue obtained after washing with methanol and drying was 4.0 g. Subjection of this residue (a brown oil) to flash chromatography (silica gel, 4:6 → 3:7 → 1:1 → 0:10 v/v petroleum ether /ethyl acetate gradient elution) afforded two fractions, A and B.

Concentration of fraction A ($R_f = 0.5$ in 3:7 v/v ethyl acetate/petroleum ether) afforded a 3:1 mixture of compounds **4** and **5** (7.4 mg) as a white, crystalline solid, m.p. = 113-128 °C. A solution of this material in methanol was allowed to stand at ambient temperatures for one week and during which time crystals formed. Subjection of one of these to single-crystal X-ray analysis revealed this to be comprised of compound **5**.

Concentration of fraction B ($R_f = 0.2$ in 3:7 v/v ethyl acetate/petroleum ether) gave compound **6** (135.3 mg) as a white, crystalline solid, m.p. = 100-113 °C (ex. methanol).

Run #2: Sand, 350 °C, 1 h. The weight of residue obtained after washing with methanol and drying was 1.4 g. Subjection of this residue to flash chromatography (silica gel, 3:7 v/v petroleum ether /ethyl acetate elution) led to the isolation of compound **6** (131.3 mg). This material was identical to that obtained from Run #1.

(b) Pyrolyses of H₃PO₄-treated Chitin.

Chitin (10.0 g) was treated with 3% H₃PO₄ (200 ml) and the resulting slurry mixed under the conditions specified below then filtered and the solids thus retained dried under the indicated conditions. The dried solid was subjected to pyrolysis in the apparatus described at Figure S5 (unless otherwise specified) above or by suspending the treated chitin in canola oil (60 mL) or using ball bearings (or without either of these). Heating of the substrate was then carried out at the indicated temperature under reduced pressure (5 mm Hg).

Run #1: Treatment of chitin with 3% aq. H₃PO₄ for 5 minutes then filtration and overnight air drying, heating at 200 °C for 3 h without ball bearings or canola oil. The weight of residue obtained after washing with methanol and drying was 171.1 mg. Subjection of the residue to reverse-phase HPLC (3:7 v/v water/acetonitrile elution)

1
2
3 afforded, after concentration of appropriate fractions, a 3:1 mixture of compounds **4** and **5**
4 (4.4 mg). This material was identical to that obtained previously.

5 **Run #2:** Treatment of chitin with 3% aq. H_3PO_4 for 5 minutes then filtration and
6 overnight air drying, heating at 200 °C in canola oil (60 ml) for 2 h. The weight of residue
7 after obtained after washing with methanol and drying was 342.1 mg. Subjection of this
8 residue to reverse-phase HPLC (3:7 v/v water/acetonitrile elution) afforded a 3:1 mixture
9 of compounds **4** and **5** (54.8 mg). This material was identical to that obtained previously.

10 **Run #3:** Treatment of chitin with 3% aq. H_3PO_4 for 48 h then filtration and overnight
11 drying in a desiccator. The resulting material was divided into three equal parts with each
12 being heated at 300 °C for 6 h in the presence of ball bearings. The combined weight of
13 the residues obtained after washing with methanol and drying was 456.6 mg. Subjection
14 of this residue to flash column chromatography (silica gel, 1.5:8.5 then 1:4 v/v ethyl
15 acetate/hexane elution) afforded three fractions, A, B and C.

16 Concentration of fraction A ($R_f = 0.5$ in 3:7 v/v ethyl acetate/petroleum ether)
17 gave a 3:1 mixture of compounds **4** and **5** (17.9 mg). This material was identical to that
18 obtained previously.

19 Concentration of fraction B ($R_f = 0.3$ in 3:7 v/v ethyl acetate/petroleum ether)
20 gave compound **9** (5.1 mg,) as a white, crystalline solid, m.p. = 64-74 °C (ex. methanol).

21 Concentration of fraction C ($R_f = 0.2$ in 3:7 v/v ethyl acetate/petroleum ether)
22 gave compound **8** (5.7 mg) as a white, crystalline solid, m.p. = 114-124 °C (ex.
23 methanol).

24 **Run #4:** Treatment of chitin with 3% aq. H_3PO_4 for 24 h then filtration and overnight
25 drying in a desiccator. Resulting material intimately mixed with acid washed and
26 chromatography grade sand then heating at 350 °C in the apparatus shown in Figure S1
27 for 1.5 h. The weight of residue obtained after washing with methanol and drying was
28 660 mg. Subjection of this residue to flash column chromatography (silica gel, 3:7 to 4:6
29 v/v ethyl acetate/petroleum ether gradient elution) afforded, after concentration of the
30 appropriate fractions, a 3:1 mixture of compounds **4** and **5** (28.5 mg). This material was
31 identical to that obtained previously.

32 **Run #5:** Chitin (10.0 g) was intimately mixed with H_3PO_4 (1.0 g of solid material) then
33 heated at 350 °C for 1.5 h using the apparatus described in Figure S1. The weight of the
34 residue obtained after washing with methanol and drying was 2.97 g. Subjection of this
35 residue to flash column chromatography (silica gel, 2:3 v/v petroleum ether/ethyl acetate
36 elution) afforded, after concentration of the appropriate fractions ($R_f = 0.2$ in 3:7 v/v ethyl
37 acetate/petroleum ether), compound **6** (87.6 mg) as a white, crystalline solid. This
38 material was identical to that obtained earlier.

39 (c) Pyrolyses of AcOH-treated Chitin.

40 Chitin (10.0 g) was treated with glacial acetic acid (150 mL) and the resulting slurry
41 heated under as detailed below then the cooled mixture was filtered and the solids thus
42 retained dried under the indicated conditions. The dried solid was subjected to pyrolysis
43 in the apparatus shown in Figure S1 and with or without acid-washed and
44 chromatography grade sand (20 g) present. The resulting mixture was heated at 350 °C
45 for 2 h.

46 **Run #1:** Chitin was heated in refluxing glacial AcOH for 3 days then the cooled
47 and filtered material was dried under a stream of air for 2 days. The resulting material
48 was heated at 350 °C for 2 h. The weight of the residue obtained after washing with
49 methanol and drying was 4.88 g. Subjection of this residue to flash chromatography
50 (silica gel, 1:1 → 6:4 v/v ethyl acetate/petroleum ether → elution) and then, in some
51 instances (as indicated by the citation of a R_f value), subjected to reverse-phase HPLC
52 (3:7 v/v water/acetonitrile elution) gave fractions A-E.

Concentration fraction A ($R_f = 0.3$ in 3:7 v/v ethyl acetate/petroleum ether and $R_t = 17.063$ min) gave compound **9** (4.9 mg), as a white, crystalline solid that was identical in all respects with the sample obtained earlier.

Concentration of fraction B [$R_f = 0.2(5)$ in 3:7 v/v ethyl acetate/petroleum ether] gave compound **6** (67.6 mg) as a white, crystalline solid that was identical in all respects with the material obtained earlier.

Concentration of fraction C [$R_f = 0.2(0)$ in 3:7 v/v ethyl acetate/petroleum ether and $R_t = 15.5$ min] gave compound **8** (6.8 mg) as a white, crystalline solid that was identical in all respects with the material obtained earlier.

Concentration of fraction D ($R_f = 0.7$ in 0.5:9.5 v/v methanol/chloroform and $R_t = 13.5$ min) gave compound **12** (4.6 mg) as a white, crystalline solid, m.p. = 124-133 °C (ex. methanol)

Concentration of fraction E ($R_f = 0.3$ in 0.5:9.5 v/v methanol/chloroform and $R_t = 17.0$ min) gave compound **13** (9.5 mg) as a white, crystalline solid, m.p. = 74-88 °C (ex. methanol).

Run #2: Chitin was stirred overnight in glacial acetic acid then filtered and air-dried before being heated at 350 °C in for 1.5 h The weight of residue (a brown oil) obtained after washing with methanol and drying was 3.57 g. This oil was to subjected to flash chromatography (silica gel, 2:3 v/v ethyl acetate/petroleum ether elution) and concentration of the relevant fractions ($R_f = 0.2$ in 3:7 v/v ethyl acetate/petroleum ether) gave compound **6** (33.9 mg) as a white, crystalline solid that was identical in all respects with the material obtained earlier.

(d) Pyrolysis of Glyoxal-treated Chitin.

Chitin (10.0 g) was treated with glyoxal (20 mL of a 40% aqueous solution) and water (30 mL). The resulting suspension was stirred for 12 h at ambient temperatures then the supernatant liquid decanted and resulting wet solid filtered under reduced pressure (Buchner funnel) and the solid thus retained dried in a desiccator. The dried and free-flowing solid was mixed with sand (20 g) and this mixture subjected to pyrolysis for 2 h at 250 °C in the apparatus shown at Figure S1. After cooling and washing the relevant parts of the apparatus with methanol, 500 mg of a brown oil was obtained. Subjection of this material to flash column chromatography (silica gel, 3:7 v/v ethyl acetate/petroleum ether elution) afforded, after concentration of the appropriate fractions ($R_f = 0.8$ in 1:1 v/v ethyl acetate/petroleum ether), levoglucosenone (9 mg). This was identical, in all respects with an authentic sample.

(e) Pyrolysis of Untreated Chitosan.

In a single run, chitosan (10.0 g) was subjected to pyrolysis, at 350 °C for 1.5 h, in the apparatus shown at Figure S1. The weight of oily residue obtained after cooling and washing the relevant parts of the apparatus with methanol and then concentrating of the ensuing solution under reduced pressure was 2.07 g. Subjection of this material to flash chromatography (silica gel, 2:8 → 10:0 v/v ethyl acetate/petroleum ether then 1:9 v/v methanol/ethyl acetate gradient elution) afforded two fractions, A and B.

Concentration of fraction A ($R_f = 0.2$ in 3:7 v/v petroleum ether/ethyl acetate) afforded compound **6** (16 mg), as a white, crystalline solid that was identical in all respects with the sample obtained earlier.

Subjection of fraction B ($R_f = 0.4$ in 1:9 v/v methanol/chloroform) to reverse-phase HPLC (3:7 v/v water/acetonitrile elution) gave three new fractions, C-E.

Concentration of fraction C ($R_f = 0.3$ in 0.5:9.5 v/v methanol/chloroform and $R_t = 7.992$ min) gave compound **14** (7.6 mg) as a white, crystalline solid, m.p. = 59-73 °C (ex. methanol).

Concentration of fraction D ($R_f = 0.4$ in 0.5:9.5 v/v methanol/chloroform and $R_t = 14.139$ min) gave compound **11** (1 mg) as a white crystalline solid, m.p. = 116-127 °C (ex. methanol).

Concentration of fraction E ($R_f = 0.2$ in 0.5:9.5 v/v methanol/chloroform and $R_t = 14.362$ min) gave compound **10** (1.5 mg) as a white, crystalline solid, m.p. = 124-133 °C (ex. methanol).

(f) Pyrolysis of Untreated and Treated NAG

Run #1: NAG (10.0 g) was subjected to pyrolysis at 350 °C for 1.5 h in the apparatus described at Figure S1. The weight of residue after washing with methanol and drying was 1.157 g. Subjection of this residue (a brown oil) to flash column chromatography (silica gel, 3:7 v/v petroleum ether/ethyl acetate elution) afforded, after concentration of the relevant fractions ($R_f = 0.2$ in 0.5:9.5 v/v methanol/chloroform), compound **10** (20.2 mg) as a white, crystalline solid that was identical, in all respects, with the sample obtained earlier.

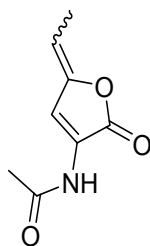
Run #2: An intimate mixture of NAG (4.4 g, 0.02 mole) and Na_2HPO_4 (2.8 g, 0.02 mole) was subjected to pyrolysis in the apparatus described at Figure S5 with stepwise heating in 50 °C increments every 0.5 h from 150 to 300 °C (total heating time 2.5 h). The weight of residue obtained after cooling and washing with methanol then drying was 562.2 mg. Subjection of this residue (a brown oil) to flash column chromatography (silica gel, 3:7 v/v petroleum ether/ethyl acetate elution) then reverse-phase HPLC (3:7 v/v water/ acetonitrile) afforded two fractions, A and B.

Concentration of fraction A ($R_f = 0.2$ in 0.5:9.5 v/v methanol/chloroform and $R_t = 13.036$ min) afforded compound **10** (6.4 mg) as a white, crystalline solid that was identical in all respects with the sample obtained earlier.

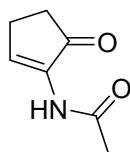
Concentration of fraction B ($R_f = 0.2$ in 0.5:9.5 v/v methanol/chloroform and $R_t = 13.445$ min) gave compound **15** (6.9 mg) as a white, crystalline solid, m.p. = 122-136 °C (ex. methanol).

Compound Characterization

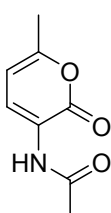
(E)- and (Z)-3-Acetamido-5-ethylidenefuran-2(5H)-one (4 and 5, respectively)



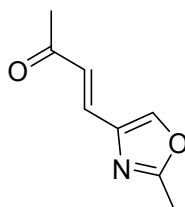
^1H NMR (400 MHz, CD_3OD) δ (major isomer) 7.51 (s, 1H), 5.34 (q, $J = 7.4$ Hz, 1H), 2.14 (s, 3H), 1.91 (d, $J = 7.4$ Hz, 3H) (resonance due to NH group proton not observed); δ (minor isomer) 7.79 (s, 1H), 5.67 (q, $J = 7.7$ Hz, 1H), 2.16 (s, 3H), 1.89 (d, $J = 7.6$ Hz, 3H) (resonance due to NH group proton not observed); $^{13}\text{C}\{^1\text{H}\}$ NMR (100 MHz, CDCl_3) δ (both isomers) 169.2, 169.0, 166.9, 149.0, 148.7, 126.2, 125.6, 120.2, 116.0, 110.9, 110.5, 106.3, 23.8, 11.9 (two resonances obscured or overlapping); IR (ATR) ν_{max} 3330, 1752, 1696, 1628, 1550, 1328, 1244, 1104, 771 cm^{-1} . MS (EI, 70 eV) m/z 167 (M^+ , 23%), 125 (100), 69 (23); HRMS (EI) m/z : (M^+) calcd for $\text{C}_8\text{H}_9\text{NO}_3$ 167.0582; Found 167.0585.

2-Acetamidocyclopent-2-en-1-one (6)¹²

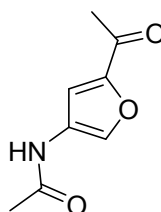
¹H NMR (400 MHz, CD₃OD) δ 7.83 (broad s, 1H), 2.61-2.67 (complex m, 2H), 2.33-2.39 (complex m, 2H), 2.10 (s, 3H) (resonance due to NH group proton not observed); ¹³C{¹H} NMR (100 MHz, CD₃OD) δ 205.3, 171.9, 143.1, 138.5, 33.1, 25.8, 23.2; IR (ATR) ν_{max} 3329, 1682, 1622, 1532, 1418, 1313, 786 cm⁻¹; MS (EI, 70 eV) *m/z* 139 (M⁺, 100%); HRMS (EI) *m/z*: (M⁺) calcd for C₇H₉NO₂ 139.0633; Found 139.0634.

3-Acetamido-6-methyl-2H-pyran-2-one (8)^{10,11}

¹H NMR (400 MHz, CD₃OD) δ 8.08 (d, *J* = 7.3 Hz, 1H), 7.80 (broad s, 1H), 6.16 (d, *J* = 7.3 Hz, 1H), 2.24 (s, 3H), 2.15 (s, 3H); ¹³C NMR (100 MHz, CD₃OD) δ 172.5, 161.4, 157.4, 128.1, 113.9, 104.7, 79.5, 23.8, 19.1. IR (ATR) ν_{max} 3337, 2925, 1713, 1681, 1643, 1420, 1338, 1110, 832, 770, 547 cm⁻¹; MS (EI, 70 eV) *m/z* 167 (M⁺, 38%), 149 (21), 125 (100), 97 (75), 96 (58); HRMS (EI) *m/z*: (M⁺) calcd for C₈H₉NO₃ 167.0582; Found 167.0584.

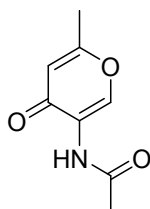
(E)-4-(2-Methyloxazol-4-yl)but-3-en-2-one (9)

¹H NMR (400 MHz, CD₃OD) δ 8.08 (s, 1H), 7.47 (d, *J* = 16.0 Hz, 1H), 6.77 (d, *J* = 16.0 Hz, 1H), 2.48 (s, 3H), 2.34 (s, 3H); ¹³C{¹H} NMR (100 MHz, CD₃OD) δ 200.8, 164.7, 142.3, 138.4, 133.1, 128.7, 27.3, 13.5; IR (ATR) ν_{max} 1670, 1638, 1362, 1266, 1239, 1104, 971, 808 cm⁻¹; MS (EI, 70 eV) *m/z* (%) 151 (M⁺, 45%), 136 (100), 109 (28), 107 (25), 80 (30); HRMS (EI) *m/z*: (M⁺) calcd for C₈H₉NO₂ 151.0633; Found 151.0635.

***N*-(5-Acetylfuran-3-yl)acetamide (10)**^{3a-c,9}

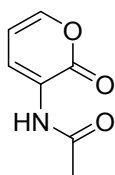
¹H NMR (400 MHz, CD₃OD) δ 8.15 (s, 1H), 7.20 (s, 1H), 2.45 (s, 3H), 2.11 (s, 3H) (resonance due to NH group proton not observed); ¹³C{¹H} NMR (100 MHz, CD₃OD) δ 188.9, 170.9, 151.9, 137.5, 128.4, 111.8, 25.8, 22.7; IR (ATR) ν_{max} 3283, 1651, 1572, 1500, 1367, 1329, 1195, 927, 768, 601 cm⁻¹; MS (EI) *m/z* 167 (M⁺, 68%), 125 (92), 110 (100); HRMS (EI) *m/z*: (M⁺) calcd for C₈H₉NO₃ 167.0582; Found 167.0583.

5-Acetamido-2-methyl-4H-pyran-4-one (11)^{10,11}



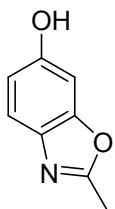
¹H NMR (400 MHz, CD₃OD) δ 9.10 (s, 1H), 6.33 (s, 1H), 2.34 (s, 3H), 2.17 (s, 3H) (resonance due to NH group proton not observed); ¹³C{¹H} NMR (100 MHz, CD₃OD) δ 174.8, 171.9, 168.8, 158.9, 147.0, 112.8, 23.3, 19.7; IR (ATR) ν_{max} 3293, 1645, 1616, 1548, 1412, 1207 cm⁻¹; MS (ESI, +ve) *m/z* 190 [(M + Na)⁺, 79%], 161 (65), 159 (100), 126 (64), 96 (64); HRMS (ESI) *m/z*: [M + Na]⁺ calcd for C₈H₉NO₃Na 190.0475; Found 190.0470.

3-Acetamido-2H-pyran-2-one (12)¹³

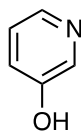


¹H NMR (400 MHz, CD₃OD) δ 8.17 (d, *J* = 7.2 Hz, 1H), 7.42 (d, *J* = 5.1 Hz, 1H), 6.39 (dd, *J* = 7.2 and 5.1 Hz, 1H), 2.17 (s, 3H) (resonance due to NH group proton not observed); ¹³C{¹H} NMR (100 MHz, CD₃OD) δ 172.7, 160.8, 146.7, 127.1, 126.0, 107.9, 23.9; IR (ATR) ν_{max} 3336, 1715, 1672, 1631, 1530, 1342, 1129, 772 cm⁻¹; MS (ESI, +ve) *m/z* 176 [(M+Na)⁺, 99%], 162 (60), 130 (100), 112 (73), 102 (73); HRMS (ESI) *m/z*: [M + Na]⁺ calcd for C₇H₇NO₃Na 176.0318; Found 176.0313.

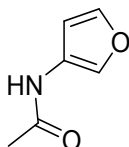
2-Methylbenzo[*d*]oxazol-6-ol (13)¹⁴



¹H NMR (400 MHz, CD₃OD) δ 7.37 (d, *J* = 8.5 Hz, 1H), 6.94 (s, 1H), 6.80 (d, *J* = 8.5 Hz, 1H), 2.56 (s, 3H) (resonance due to OH group proton not observed); ¹³C{¹H} NMR (100 MHz, CD₃OD) δ 157.1, 126.1, 119.7, 113.9, 112.6, 110.6, 98.1, 14.0; IR (ATR) ν_{max} 3236, 1621, 1486, 1451, 1299, 1137, 1110 cm⁻¹; MS (ESI, +ve) *m/z* 150 [(M + H)⁺, 100%], 130 (48), 102 (40), 91 (44), 74 (39); HRMS (ESI) *m/z*: [M + H]⁺ calcd for C₈H₈NO₂ 150.0544; Found 150.0550.

Pyridin-3-ol (14)¹⁵

This compound could only be characterized by single-crystal X-ray analysis (details presented below).

N-(Furan-3-yl)acetamide (15)¹¹

¹H NMR (400 MHz, CD₃OD) δ 7.90 (s, 1H), 7.36 (broad s, 1H), 6.37 (broad s, 1H), 2.08 (s, 3H) (resonance due to NH group proton not observed); ¹³C{¹H} NMR (100 MHz, CD₃OD) δ 170.6, 142.7, 133.4, 126.1, 105.6, 22.7; IR (ATR) ν_{max} 3278, 1657, 1563, 1378, 1289, 1166, 870, 765 cm⁻¹; MS (EI, 70 eV) *m/z* 125 (M⁺, 88%), 83 (100), 69 (29); HRMS (EI) *m/z*: (M⁺) calcd for C₆H₇NO₂ 125.0477; Found 125.0479.

Crystallographic Studies.**Crystallographic Data.**

Compound **5**. C₈H₉NO₃, *M* = 167.16, *T* = 150 K, triclinic, space group *P* $\bar{1}$, *Z* = 2, *a* = 4.6446(8) Å, *b* = 8.456(2) Å, *c* = 10.7100(16) Å; α = 89.422(18)°, β = 86.974(13)°, γ = 80.489 (18)°; *V* = 414.27(14) Å³, *D_x* = 1.340 Mg m⁻³, 1635 unique data (2θ_{max} = 147°), *R* = 0.087 [for 1222 reflections with *I* > 2.0σ(*I*)]; *R_w* = 0.266 (all data), *S* = 1.06.

Compound **6**. C₇H₉NO₂, *M* = 139.15, *T* = 150 K, monoclinic, space group *C*2/*c*, *Z* = 8, *a* = 18.5157(10) Å, *b* = 9.4421(5) Å, *c* = 7.9012(4) Å; α = 90°, β = 101.918(5)°, γ = 90°; *V* = 1351.57(13) Å³, *D_x* = 1.368 Mg m⁻³, 1519 unique data (2θ_{max} = 58.446°), *R* = 0.0572 [for 1263 reflections with *I* > 2.0σ(*I*)]; *R_w* = 0.1168 (all data), *S* = 1.061.

Compound **8**. C₈H₉NO₃, *M* = 167.16, *T* = 150 K, triclinic, space group *P* $\bar{1}$, *Z* = 2, *a* = 6.9199(4) Å, *b* = 7.5328(5) Å, *c* = 7.9552(5) Å; α = 96.283(6)°, β = 97.670(5)°, γ = 109.017(6)°; *V* = 383.32(2) Å³, *D_x* = 1.448 Mg m⁻³, 1538 unique data (2θ_{max} = 147.4°), *R* = 0.054 [for 1469 reflections with *I* > 2.0σ(*I*)]; *R_w* = 0.152 (all data), *S* = 1.00.

Compound **9**. C₈H₁₃NO₄, *M* = 187.19, *T* = 150 K, monoclinic, space group *I*2/*m*, *Z* = 4, *a* = 5.6345(4) Å, *b* = 6.4841(5) Å, *c* = 25.9775(17) Å; α = 90°, β = 95.661(7)°, γ = 90°; *V* = 944.44(12) Å³, *D_x* = 1.317 Mg m⁻³, 1159 unique data (2θ_{max} = 57.714°), *R* = 0.0167 [for 1034 reflections with *I* > 2.0σ(*I*)]; *R_w* = 0.1044 (all data), *S* = 1.060.

Compound **10**. C₈H₁₁NO₄, *M* = 185.18, *T* = 150 K, monoclinic, space group *P*2₁/*c*, *Z* = 4, *a* = 6.160(4) Å, *b* = 11.4782(5) Å, *c* = 11.3108(5) Å; α = 90°, β = 102.768(5)°, γ = 90°; *V* = 863.02 (8) Å³, *D_x* = 1.425 Mg m⁻³, 2066 unique data (2θ_{max} = 58.316°), *R* = 0.0604 [for 1389 reflections with *I* > 2.0σ(*I*)]; *R_w* = 0.1480 (all data), *S* = 1.080.

Compound **11**. C₈H₉NO₃, *M* = 167.16, *T* = 150 K, triclinic, space group *P*-1, *Z* = 2, *a* = 3.8928(10) Å, *b* = 9.3628(16) Å, *c* = 10.7006(14) Å; α = 81.053(12)°, β = 83.731(16)°, γ = 79.026°; *V* = 376.94 (13) Å³, *D_x* = 1.473 Mg m⁻³, 1486 unique data (2θ_{max} = 147.304°), *R* = 0.0649 [for 1141 reflections with *I* > 2.0σ(*I*)]; *R_w* = 0.1760 (all data), *S* = 1.029.

Compound **12**. C₇H₇NO₃, *M* = 153.14, *T* = 150 K, triclinic, space group *P*-1, *Z* = 2, *a* = 3.7878(3) Å, *b* = 9.6277(8) Å, *c* = 10.3407(8) Å; α = 63.995(8)°, β = 84.352(7)°, γ =

80.203(7)°; $V = 333.86(5) \text{ \AA}^3$, $D_x = 1.523 \text{ Mg m}^{-3}$, 1337 unique data ($2\theta_{\text{max}} = 146.992^\circ$), $R = 0.0362$ [for 1192 reflections with $I > 2.0\sigma(I)$]; $R_w = 0.0985$ (all data), $S = 1.051$.

Compound **13**. $\text{C}_8\text{H}_7\text{NO}_2$, $M = 149.15$, $T = 150 \text{ K}$, triclinic, space group $P-1$, $Z = 2$, $a = 6.5474(7) \text{ \AA}$, $b = 7.2418(7) \text{ \AA}$, $c = 7.6043(7) \text{ \AA}$; $\alpha = 77.401(8)^\circ$, $\beta = 85.073(8)^\circ$, $\gamma = 78.699(9)^\circ$; $V = 344.70(6) \text{ \AA}^3$, $D_x = 1.437 \text{ Mg m}^{-3}$, 1378 unique data ($2\theta_{\text{max}} = 147.654^\circ$), $R = 0.0450$ [for 1124 reflections with $I > 2.0\sigma(I)$]; $R_w = 0.1211$ (all data), $S = 1.051$.

Compound **14**. $\text{C}_7\text{H}_6\text{F}_3\text{NO}_3$, $M = 209.13$, $T = 150 \text{ K}$, triclinic, space group $P-1$, $Z = 2$, $a = 6.2250(14) \text{ \AA}$, $b = 7.862(3) \text{ \AA}$, $c = 8.7433(18) \text{ \AA}$; $\alpha = 103.85(2)^\circ$, $\beta = 94.753(18)^\circ$, $\gamma = 95.55(2)^\circ$; $V = 4.11.04(19) \text{ \AA}^3$, $D_x = 1.690 \text{ Mg m}^{-3}$, 1393 unique data ($2\theta_{\text{max}} = 133.192^\circ$), $R = 0.0856$ [for 788 reflections with $I > 2.0\sigma(I)$]; $R_w = 0.2456$ (all data), $S = 1.024$.

Compound **15**. $\text{C}_6\text{H}_7\text{NO}_2$, $M = 125.13$, $T = 150 \text{ K}$, orthorhombic, space group $Pbca$, $Z = 8$, $a = 9.6520(4) \text{ \AA}$, $b = 9.3307(5) \text{ \AA}$, $c = 13.2182(6) \text{ \AA}$; $V = 1190.43(10) \text{ \AA}^3$, $D_x = 1.396 \text{ Mg m}^{-3}$, 1199 unique data ($2\theta_{\text{max}} = 147.496^\circ$), $R = 0.0464$ [for 1073 reflections with $I > 2.0\sigma(I)$]; $R_w = 0.1330$ (all data), $S = 1.082$.

Structure Determinations.

Data for compound **5**, **6**, **8**, **9** and **11-15** were measured on a Rigaku SuperNova diffractometer using $\text{CuK}\alpha$, graphite monochromator ($\lambda = 1.54184 \text{ \AA}$) while data for compound **10** were measured on the same machine using a $\text{MoK}\alpha$, graphite monochromator ($\lambda = 0.71073 \text{ \AA}$). Data collection, cell refinement and data reduction employed the CrysAlis PRO program²⁵ while SHELXT²⁶ and SHELXL²⁷ were used for structure solution and refinement. Atomic coordinates, bond lengths and angles, and displacement parameters have been deposited at the Cambridge Crystallographic Data Centre (CCDC nos. 1935464-1935469). These data can be obtained free-of-charge via www.ccdc.cam.ac.uk/data_request/cif, by emailing data_request@ccdc.cam.ac.uk, or by contacting The Cambridge Crystallographic Data Centre, 12 Union Road, Cambridge CB2 1EZ, UK; fax: +44 1223 336033.

Accession Codes

CCDC depositions 1943032-1943041 contain the supplementary crystallographic data for this paper. These data can be obtained free of charge via www.ccdc.cam.ac.uk/data_request/cif, or by e-mailing data_request@ccdc.cam.ac.uk, or by contacting The Cambridge Crystallographic Data Centre, 12 Union Road, Cambridge CB2 1EZ, U.K.; fax: +44 1223 336033.

THEORETICAL STUDIES

Methodologies

Geometries were optimized at the M06-2X/6-31+G(d) level of theory²⁸ and frequencies were also calculated at this level. Geometries were verified either as local minima or transition states. Entropies, thermal corrections, and zero-point vibrational energies were scaled using the recommended scaling factors.²⁹ Single-point energies were calculated using the high-level composite ab initio method G3(MP2,CC) to improve accuracy.³⁰ For all species investigated, conformational searching was performed with the energy-directed tree search (EDTS) algorithm³¹ to identify conformations with the lowest Gibbs free-energy. All standard ab initio molecular orbital theory and density functional theory (DFT) calculations were carried out using the Gaussian 09³² and Molpro 2015³³ software packages.

Outcomes

The mechanisms for the conversion of compound **21** into **22** (Scheme S1) and **23** into **24** (Scheme S2) were studied using high-level ab initio molecular orbital theory calculations. A variety of reaction pathways was considered and the most energetically feasible ones

1
2
3 are shown. In both transformations, deprotonation of the tertiary OH associated with the
4 oxazolidine ring triggers ring opening, affording the first intermediate (**INT 1**) that upon
5 re-protonation provides a species (**INT 2**) that can itself undergo a hydride shift
6 accompanied by a concerted C–O bond cleavage. The resulting intermediate (**INT 3**) can
7 then lose water to afford compound **22**. An analogous pathway appears to operate in the
8 case of the conversion **23** → **24**. In both cases the rate determining hydride shift is highly
9 exergonic ($\Delta G = -403.1 \text{ kJ mol}^{-1}$ and $-331.5 \text{ kJ mol}^{-1}$), and proceeds with experimentally
10 accessible barriers of 84.3 kJ mol^{-1} and $111.1 \text{ kJ mol}^{-1}$ for the processes leading to
11 products **22** and **24**, respectively.
12
13

14 ASSOCIATED CONTENT

15 Supporting Information

16 The Supporting Information is available free-of-charge on the ACS Publications website
17 at DOI: 10.1021/acs.joc.XXXXXX.
18

19 Experimental procedures, spectroscopic data, copies of the NMR spectra of
20 compounds **4-13** and **15**, X-ray data and derived ORTEPs for pyrolysis products
21 **5-15**, theoretical studies of key aspects of the mechanisms shown in Schemes 2
22 and 3 together with full details of the calculations and raw computational data.
23
24
25

26 AUTHOR INFORMATION

27 Corresponding Author

28 *E-mail: Martin.Banwell@anu.edu.au

29 ORCID

30 Martin G. Banwell: [0000-0002-0582-475X](https://orcid.org/0000-0002-0582-475X)

31 Michelle Coote: 0000-0003-0828-7053

32 Jiri Mikusek: 0000-0001-5425-0193

33 Author Contributions

34 The manuscript was written through contributions from all of the authors. All of the
35 authors have given approval to the final version of the manuscript.
36

37 Notes

38 The authors declare no competing financial interest.
39
40

41 ACKNOWLEDGEMENTS

42 We thank the Australian Government and Circa Pty Ltd for the provision of an
43 Innovations Connections grant. Funding from the Australian Research Council is
44 gratefully acknowledged (including through grants FL170100041 and CE140100012) as
45 is support (to MN) from the Islamic Government of Iran. Dr Hideki Onagi (RSC) and Mr
46 Daniel Barktus (RSC) are thanked for outstanding technical assistance.
47
48
49
50
51
52
53

54 REFERENCES

- 55 1. Yan, N.; Chen, X. Don't Waste Seafood Waste, *Nature*, **2015**, *524*, 155-158 and
56 references cited therein.
- 57 2. Lie, Y.; Ortiz, P.; Vendamme, R.; Vanbroekhoven, K.; Farmer, T. J.
58 *BioLogicTool*: A Simple Visual Tool for Assisting in the Logical Selection of
59
60

- 1
2
3 Pathways from Biomass to Products. *Ind. Eng. Chem. Res.* **2019**, *58*, 15945-
4 15957.
- 5
6 3. For some representative reports, see: (a) Chen, J.; Wang, M.; Ho, C.-T. Volatile
7 Compounds Generated from Thermal Degradation of *N*-Acetylglucosamine. *J.*
8 *Agric. Food Chem.* **1998**, *46*, 3207-3209; (b) Drover, M. W.; Omari, K. W.;
9 Murphy, J. N.; Kerton, F. M. Formation of a Renewable Amide, 3-Acetamido-5-
10 acetylfuran, via Direct Conversion of *N*-Acetyl-D-glucosamine. *RSC Advances*,
11 **2012**, *2*, 4642-4644; (c) Chen, X.; Gao, Y.; Wang, L.; Chen, H.; Yan, N. Effect of
12 Treatment Methods on Chitin Structure and its Transformation into Nitrogen-
13 Containing Chemicals. *ChemPlusChem* **2015**, *80*, 1565-1572; (d) Gao, X.; Chen,
14 X.; Zhang, J.; Guo, W.; Jin, F.; Yan, N. Transformation of Chitin and Waste
15 Shrimp Shells into Acetic Acid and Pyrrole. *ACS Sustainable Chem. Eng.* **2016**, *4*,
16 3912-3920; (e) Liu, C.; Zhang, H.; Xiao, R.; Wu, S. Value-Added Organonitrogen
17 Chemicals Evolution from Pyrolysis of Chitin and Chitosan. *Carbohydrate*
18 *Polymers*, **2017**, *156*, 118-124; (f) Hülsey, M. J.; Yang, H.; Yan, N. Sustainable
19 Routes for the Synthesis of Renewable Heteroatom-Containing Chemicals. *ACS*
20 *Sustainable Chem. Eng.* **2018**, *6*, 5694-5707; (g) Zhang, P.; Hu, H.; Tang, H.;
21 Yang, Y.; Liu, H.; Lu, Q.; Li, X.; Worasuwannarak, N.; Yao, H. In-depth
22 Experimental Study of Pyrolysis Characteristics of Raw and Cooking Treated
23 Shrimp Shell Samples. *Renewable Energy*, **2019**, *139*, 730-738.
- 24
25 4. See, for example: (a) Liu, Y.; Stähler, C.; Murphy, J. N.; Furling, B. J.; Kerton, F.
26 M. Formation of a Renewable Amine and an Alcohol via Transformations of 3-
27 Acetamido-5-acetylfuran. *ACS Sustainable Chem. Eng.* **2017**, *5*, 4916-4922; (b)
28 Pham, T. T.; Chen, X.; Yan, N.; Sperry, J. A Novel Dihydrodifuropyridine
29 Scaffold Derived from Ketones and the Chitin-derived Heterocycle 3-Acetamido-
30 5-acetylfuran. *Monatsh Chem.* **2018**, *149*, 857-861; (c) Sadiq, A. D.; Chen, X.;
31 Yan, N.; Sperry, J. Towards the Shell Biorefinery: Sustainable Synthesis of the
32 Anticancer Alkaloid Proximicin A from Chitin. *ChemSusChem* **2018**, *11*, 532-
33 535; (d) Pham, T. T.; Gözaydin, G.; Söhnel, T.; Yan, N.; Sperry, J. Oxidative
34 Ring-Expansion of a Chitin-Derived Platform Enables to Unexplored 2-Amino
35 Sugar Chemical Space. *Eur. J. Org. Chem.* **2019**, 1355-1360.
- 36
37 5. (a) Ma, X., Anderson, N., White, L. V., Bae, S., Raverty, W., Willis, A. C. and
38 Banwell, M. G. The Conversion of Levoglucosenone into Isolevoglucosenone.
39 *Aust. J. Chem.* **2015**, *68*, 593-599; (b) Ma, X., Liu, X., Yates, P., Rafferty, W.,
40 Banwell, M. G., Ma, C., Willis, A. C., Carr, P. D. Manipulating the Enone Moiety
41 of Levoglucosenone: 1,3-Transposition Reactions Including Ones Leading to
42 Isolevoglucosenone. *Tetrahedron* **2018**, *74*, 5000-5011.
- 43
44 6. (a) Wang, Z.; Lu, Q.; Zhu, X.-F.; Zhang, Y. Catalytic Fast Pyrolysis of Cellulose
45 to Prepare Levoglucosenone Using Sulfated Zirconia. *ChemSusChem*, **2011**, *4*,
46 79-84; (b) Kudo, S.; Goto, N.; Sperry, J.; Norinaga, K.; Hayashi, J.-i. Production
47 of Levoglucosenone and Dihydrolevoglucosenone by Catalytic Reforming of
48 Volatiles from Cellulose Pyrolysis Using Supported Ionic Liquid Phase. *ACS*
49 *Sustainable Chem. Eng.* **2017**, *5*, 1132-1140 and references cited therein.
- 50
51 7. (a) Camp, J. E. Bio-available Solvent Cyrene: Synthesis, Derivatization and
52 Applications. *ChemSusChem*. **2018**, *11*, 3048-3055. (b) <https://cen.acs.org/business/biobased-chemicals/New-solvent-Cyrene-takes-NMP/97/i22> (accessed 07/05/
53 2019).
- 54
55 8. A range of experiments was undertaken in an effort to promote heat transfer to the
56 substrate (viz. to the chitin, chitosan or NAG). These included placing ball
57 bearings inside the vessel and stirring the contents magnetically, using mixtures of
58
59
60

- the substrate with acid washed sand and suspensions of the substrate in canola oil. Details are provided in the SI.
9. Zhu, H.-J.; Yan, Y.-M.; Tu, Z.-C.; Luo, J.-F.; Liang, R.; Yang, T.-H.; Cheng, Y.-X.; Wang, S.-M. Compounds from *Polyphaga plancyi* and their Inhibitory Activities Against JAK3 and DDR1 Kinases. *Fitoterapia*, **2016**, *114*, 163-167.
 10. Franich, R. A.; Goodin, S. J.; Wilkins, A. L. Acetamidofurans, Acetamidopyrones, and Acetamidoacetaldehyde from Pyrolysis of Chitin and *N*-Acetylglucosamine, *J. Anal. Appl. Pyrolysis*, **1984**, *7*, 91-100.
 11. Staniewicz, B. A.; Mastalerz, M.; Hof, C. H. J.; Bierstedt, A.; Flannery, M. G.; Briggs, D. E. G.; Evershed, R. P. Biodegradation of the Chitin-Protein Complex in Crustacean Cuticle. *Org. Geochem.* **1998**, *28*, 67-76.
 12. Effenberger, F.; Beisswenger, T.; Az, R. Decomposition of 2-Azido Ketones to 2-(Acetylamino)-2-alken-1-ones by Perrhenate Catalysis. *Chem. Ber.* **1985**, *118*, 4869-4876.
 13. Nin, A.P.; de Lederkremer, R. M.; Varela, O. Synthesis of (2*S*, 4*R*, 5*R*)-4,5,6-Trihydroxynorleucine and 5-Hydroxynorvaline from Precursors Obtained by an Unusual Rearrangement in a 5,6-Dihydro-2-pyrone. *Tetrahedron*, **1996**, *52*, 12911-12918.
 14. Schreiner, E. P.; Wolff, B.; Winiski, A. P.; Billich, A. 6-(2-Adamantan-2-ylidene-hydroxybenzoxazole)-*O*-sulfamate. A Potent Non-steroidal Irreversible Inhibitor of Human Steroid Sulfatase. *Bioorg. Med. Chem. Lett.* **2003**, *13*, 4313-4316.
 15. Caprio, V. 7.03 - Pyridines and their Benzo Derivatives: Reactivity of Substituents. *Comprehensive Heterocyclic Chemistry III*. **2008**, *7*, 101-169.
 16. Denmark, S. E.; Jaunet, A. Catalytic, Enantioselective, Intramolecular Carbosulfenylation of Olefins. Preparative and Stereochemical Aspects. *J. Org. Chem.* **2014**, *79*, 140-171 and references cited there-in.
 17. For useful commentaries on such processes, see: (a) Boelma, E.; Wieringa, J. H.; Wynberg, H.; Starting, J. An Intramolecular 1,3-Hydride Shift in the Adamantane Series. *Tetrahedron Lett.* **1973**, 2377-2380; (b) Faraldos, J. A.; Wu, S.; Chappl, J.; Coates, R. M. Doubly Labeled Patchouli Alcohol from Singly Labeled [2-²H₁]Farnesyl Diphosphate Catalyzed by Recombinant Patchouli Synthase. *J. Am. Chem. Soc.* **2010**, *132*, 2998-3008; (c) Assary, R. S.; Curtiss, L. A. Comparison of Sugar Molecule Decomposition through Glucose and Fructose. A High-Level Quantum Chemical Study. *Energy & Fuels*, **2012**, *26*, 1344-1352; (d) Rinkel, J.; Rabe, P.; Garbeva, P.; Dickschat, J. S. Lessons from 1,3-Hydride Shifts in Sesquiterpene Cyclizations. *Angew. Chem. Int. Ed.* **2016**, *55*, 13593-13596.
 18. These dehydration processes could also involve direct elimination of the elements of water across two conjoined carbons or a cyclodehydration process leading to an intermediate epoxide that rearranges to the corresponding aldehyde or ketone.
 19. Novotny, O.; Cejpek, K.; Velisek, J. Formation of α -Hydroxy and α -Dicarbonyl Compounds during Degradation of Monosaccharides. *Czech J. Food Sci.* **2007**, *25*, 119-130.
 20. Clearly the pre-treatment of chitin with glyoxal failed to enhance the production of compound **9** (see Entry 4, Table 1).
 21. This possible mode of deoxygenation of vicinal diols is one we are currently exploring, especially through pyrolysis of the derived Ley acetals.
 22. Bogart, J. W.; Bowers, A. A. Dehydroamino acids: Chemical Multi-tools for Late-stage Diversification. *Org. Biomol. Chem.* **2019**, *17*, 3653-3669 and references cited therein.

- 1
2
3
4
5
6
7
8
9
10
11
12
13
14
15
16
17
18
19
20
21
22
23
24
25
26
27
28
29
30
31
32
33
34
35
36
37
38
39
40
41
42
43
44
45
46
47
48
49
50
51
52
53
54
55
56
57
58
59
60
23. Still, W. C.; Kahn, M.; Mitra, A. Rapid Chromatographic Technique for Preparative Separations with Moderate Resolution. *J. Org. Chem.*, **1978**, *43*, 2923–2925.
 24. Pangborn, A. B.; Giardello, M. A.; Grubbs, R. H.; Rosen, R. K.; Timmers, F. J. Safe and Convenient Procedure for Solvent Purification. *Organometallics*, **1996**, *15*, 1518–1520.
 25. CrysAlis PRO Version 1.171.37.35h (release 09-02-2015 CrysAlis171.NET) (compiled Feb 9 2015, 16:26:32) Agilent Technologies: Oxfordshire, UK.
 26. Sheldrick, G. M. SHELXT – Integrated Space-Group and Crystal-Structure Determination. *Acta Cryst.* **2015**, *A71*, 3-8.
 27. Sheldrick, G. M. Crystal Structure Refinement with SHELXL. *Acta Cryst.* **2015**, *C71*, 3-8.
 28. Zhao, Y.; Truhlar, D. G., The M06 suite of density functionals for main group thermochemistry, thermochemical kinetics, noncovalent interactions, excited states, and transition elements: two new functionals and systematic testing of four M06-class functionals and 12 other functionals. *Theoretical Chemistry Accounts* **2008**, *120*, 215-241.
 29. Alecu, I.; Zheng, J.; Zhao, Y.; Truhlar, D. G., Computational thermochemistry: scale factor databases and scale factors for vibrational frequencies obtained from electronic model chemistries. *Journal of chemical theory and computation* **2010**, *6*, 2872-2887.
 30. Curtiss, L. A.; Raghavachari, K.; Redfern, P. C.; Baboul, A. G.; Pople, J. A., Gaussian-3 theory using coupled cluster energies. *Chemical Physics Letters* **1999**, *314*, 101-107.
 31. Izgorodina, E. I.; Lin, C. Y.; Coote, M. L., Energy-directed tree search: an efficient systematic algorithm for finding the lowest energy conformation of molecules. *Physical Chemistry Chemical Physics* **2007**, *9*, 2507-2516.
 32. Frisch, M.; Trucks, G.; Schlegel, H.; Scuseria, G.; Robb, M.; Cheeseman, J.; Scalmani, G.; Barone, V.; Petersson, G.; Nakatsuji, H.; et al., Gaussian 09. Revision E. 01. Gaussian Inc., Wallingford, CT, USA. **2009**.
 33. Werner, H.; Knowles, P.; Knizia, G.; Manby, F.; Schütz, M.; Celani, P.; Györffy, W.; Kats, D.; Korona, T.; Lindh, R.; et al., MOLPRO, Version 2015.1, a Package of ab initio Programs. **2015**.